Advances in Brief

Increased Uptake of the Apoptosis-imaging Agent ^{99m}Tc Recombinant Human Annexin V in Human Tumors after One Course of Chemotherapy as a Predictor of Tumor Response and Patient Prognosis[1]

Tarik Belhocine,[2] Neil Steinmetz, Roland Hustinx, Pierre Bartsch, Guy Jerusalem, Laurence Seidel, Pierre Rigo, and Allan Green

Division of Nuclear Medicine [T. B., R. H., P. R.], Pneumology [P. B.], Oncology [G. J.], and Biostatistics and Epidemiology [L. S.], University Hospital of Liège, 4000 Liège, Belgium, and Theseus Imaging Corporation, Boston, Massachusetts 02111 [N. S., A. G.]

Abstract

Purpose: **Many anticancer therapies exert their therapeutic effect by inducing apoptosis in target tumors. We evaluated in a Phase I study the safety and the feasibility of ^{99m}Tc-Annexin V for imaging chemotherapy-induced apoptosis in human cancers immediately after the first course of chemotherapy.**

Experimental Design: **Fifteen patients presenting with lung cancer ($n = 10$), lymphoma ($n = 3$), or breast cancer ($n = 2$) underwent ^{99m}Tc-Annexin V scintigraphy before and within 3 days after their first course of chemotherapy. Tumor response was evaluated by computed tomography and ^{18}F-fluoro-2-deoxy-D-glucose positron emission tomography scans, 3 months in average after completing the treatment. Median follow-up was 117 days.**

Results: **In all cases, no tracer uptake was observed before treatment. However, 24–48 h after the first course of chemotherapy, 7 patients who showed ^{99m}Tc-Annexin V uptake at tumor sites, suggesting apoptosis, had a complete ($n = 4$) or a partial response ($n = 3$). Conversely, 6 of the 8 patients who showed no significant posttreatment tumor uptake had a progressive disease. Despite the lack of tracer uptake after treatment, the 2 patients with breast cancer had a partial response. Overall survival and progression-free survival were significantly related to tracer uptake in treated lung cancers and lymphomas ($P < 0.05$). No serious adverse events were observed.**

Conclusions: **Our preliminary results demonstrated the feasibility and the safety of ^{99m}Tc-Annexin V for imaging apoptosis in human tumors after the first course of chemotherapy. Initial data suggest that early ^{99m}Tc-Annexin V tumor uptake may be a predictor of response to treatment in-patients with late stage lung cancer and lymphoma.**

Introduction

The molecular basis of cancer is now widely believed to involve mutations that lead to deregulated cellular proliferation and suppression mechanisms controlling programmed cell death (1, 2). For instance, mutations of the powerful apoptosis-inducing *myc* protein or the loss of *p53* protein function have been shown to play a crucial role in carcinogenesis (3). Tumor sensitivity to any given therapeutic regimen commonly is mediated by the initiation of programmed cell death via available active apoptotic pathways. Many therapeutically effective anticancer drugs act to interfere with DNA synthesis and cell division, thereby inducing apoptosis in susceptible target tumors (4, 5). Thus, it may be possible to determine the effectiveness of a proposed anticancer regimen on a patient-by-patient basis by assessing the degree of apoptosis in target tumors soon after the initial treatment.

Recombinant human Annexin V (rh-Annexin V)[3] has been shown to bind with high avidity to PS, a membrane-associated intracellular phospholipid invariably expressed on the external cell membrane surface early in the apoptotic cascade (6). Fluorescein-labeled rh-Annexin V has been widely used as a histopathological marker of apoptosis. More recently, radiolabeled rh-Annexin V has been shown to provide noninvasive imaging of programmed cell death in animal models associated with Fas administration, organ transplant rejection, neonatal hypoxic brain injury, terminal differentiation of WBCs associated with inflammation, and cytoxan treatment of murine lymphoma (7–14). Similarly, radiolabeled rh-Annexin V was successfully used for localizing apoptosis in human diseases such as myocardial infarction and cardiac allograft rejection (15, 16).

To assess the potential of such an imaging agent to demonstrate treatment-induced apoptosis as an early predictor to

Received 2/14/02; revised 4/17/02; accepted 4/19/02.
The costs of publication of this article were defrayed in part by the payment of page charges. This article must therefore be hereby marked *advertisement* in accordance with 18 U.S.C. Section 1734 solely to indicate this fact.
[1] Supported by research grant from Theseus Imaging Corporation (Boston, MA). Presented in part at the 47th annual meeting of the Society of Nuclear Medicine (St. Louis, MO, June 2000).
[2] To whom requests for reprints should be addressed, at Division of Nuclear Medicine, University Hospital of Liège, Sart Tilman, Bât.35, 4000 Liège, Belgium. Phone: 32-04-366-71-99; Fax: 32-04-366-79-33; E-mail: tarik.bel@swing.be.

[3] The abbreviations used are: rh-Annexin V, recombinant human Annexin V; PS, phosphatidylserine; CT, computed tomography; SPECT, single-photon emission computed tomography; TBR, tumor-to-background ratio; ROI, regions of interest; TR, tumor ratio; ^{18}FDG, ^{18}F-fluoro-2-deoxy-D-glucose; PET, positron emission tomography; NHL, non-Hodgkin's lymphoma; HL, Hodgkin's lymphoma; NSCLC, non-small cell lung cancer; SCLC, small cell lung cancer; AI, apoptotic index; CR, complete remission; PR, partial remission; PD, progressive disease.

Table 1 Patient characteristics

Cases	Gender	Age (yr)	Tumor histology (stage)	Chemotherapy drugs
1	Male	65	SCLC (IV)	MIP[a]-VP16
2	Male	69	NSCLC (IV)	MIP
3	Male	67	NHL (IV)	CHOP
4	Male	69	NSCLC (IV)	MIP
5	Male	80	NSCLC (IV)	MIP
6	Female	69	BC (III)	T
7	Female	68	NSCLC (IV)	MIP
8	Female	61	BC (III)	T
9	Male	68	NSCLC (IV)	MIP
10	Male	42	NSCLC (IV)	MIP
11	Male	33	NSCLC (IV)	MIP
12	Male	56	NHL (IV)	MCE
13	Female	45	HL (II)	ABVD
14	Male	56	SCLC (III)	C-VP16
15	Male	53	SCLC (III)	P-VP16

[a] MIP, mitomycin-ifosfamide-*cis*-platinum; VIP, vepeside; CHOP, cyclophosphamide-doxorubicine-vincristine-prednisone; T, taxane; MCE, melphalan-cyclolal-endoxan; ABVD, adriamycin-bleomycin-vincristine-doxorubicine; C, carboplatine; BC, breast cancer.

anticancer treatment, patients initiating chemotherapy for stage III or IV SCLC and NSCLC, breast cancer or lymphoma was prospectively studied with a newly developed nuclear medicine imaging agent, Technetium Tc-99m rh-Annexin V (Apomate). Subjects were imaged before initiation of chemotherapy and immediately after one course of chemotherapy for evaluating the ability of the radiopharmaceutical to visualize apoptosis posttreatment in comparison to baseline. In addition, patients were followed up for 1 year to correlate the occurrence of detectable increases in tumor cell death 24 to 48 h after completing the first course of chemotherapy with tumor response to treatment, time to progression of disease, and survival time.

Patients and Methods

Patients. Fifteen patients (11 male and 4 female; mean age = 60 years) scheduled for chemotherapy of histologically confirmed NSCLC ($n = 7$), SCLC ($n = 3$), NHL ($n = 2$), HL ($n = 1$), or disseminated breast cancer ($n = 2$) were enrolled in this study. All patients were at least 18 years of age and clinically stable with a baseline Karnofsky Performance Status score of at least 70 and a minimum estimated life expectancy of 16 weeks. Patients were considered eligible if they had one or more extra-abdominal bidimensionally measurable lesions on an imaging study (X-ray, CT, ultrasonography, or magnetic resonance imaging) at least 1 cm in the longest diameter. All patients signed an informed consent form at moment of recruitment. Patient characteristics are summarized in Table 1.

Biochemical Basis for the Imaging of Apoptosis. The externalization of PS from the inner leaflet to the outer leaflet of the cell membrane is an universal feature occurring within 90–120 min of apoptotic signalizing "*in vitro*," before membrane bleb formation and DNA degradation (6, 17). Annexin V, a human protein with a molecular weight 36,000 (18, 19), which is physiologically found in the cytoplasm of a wide variety of cell types, including placental, endothelial and smooth muscle cells, is known to have a high affinity for cells with exposed PS *in vitro* and *in vivo* (20, 21).

Preparation of ^{99m}Tc rh-Annexin V. rh-Annexin V produced in *Escherichia coli* was labeled using a kit (Apomate; Theseus Imaging Corporation, Boston, MA) based on the preformed ^{99m}Tc phentioate ligand method described by Kasina and Fritzberg (22). A radiochemical purity of ≥85% determined by instant thin layer chromatography was required before injecting the radiolabeled tracer.

^{99m}Tc rh-Annexin V Imaging Procedure. All patients enrolled in the study were evaluated with physical examination and laboratory studies (chemistries, hematology, coagulation, routine analysis, and vital signs) before injection of the imaging agent as well as after administration of ^{99m}Tc rh-Annexin V. The protocol design is summarized in Fig. 1.

Fifteen to 30 mCi of ^{99m}Tc rh-Annexin V were administered i.v. slowly over 3–5 min. According to the study protocol, all patients underwent ^{99m}Tc rh-Annexin V scintigraphy, including planar anterior and posterior thoracic views of all measurable tumor masses at 3–6 and 24 h after tracer injection (before and after the first course of chemotherapy). Eleven patients had also dynamic sequences and whole body images immediately and 3–6 h, respectively, after ^{99m}Tc rh-Annexin V administration. Two patients had an optional SPECT acquisition 4 h after tracer injection.

Annexin V imaging was performed using a large field of view camera fitted with a low energy, parallel hole, high resolution collimator. Dynamic images were collected for 10 min after injection (20 s/frame); planar studies were acquired in a 256 × 256 matrix; anterior and posterior whole body images were obtained at a scan speed of 10 cm/min; SPECT data acquisition was obtained using a 128 × 128 matrix with a complete rotation of 360°. A minimum number of counts/images and 250,000 counts/image were collected for the planar image performd at the 3–6-h and 24-h, respectively. SPECT images were reconstructed using an iterative method based on an Ordered Subset–Expectation Maximization principle.

Image Interpretation. Qualitative assessment of tumor uptake was performed using visual reading of the Apomate images by two nuclear physicians blinded to tumor response to chemotherapy. Except for physiological distribution of tracer, any Annexin V-Tc^{99m} uptake detected immediately after chemotherapy at tumor sites and not seen on the pretreatment images was considered as a positive result. Otherwise, in the absence of posttreatment tumor uptake of the apoptosis agent, the case was then interpreted as a negative result.

Semiquantitative evaluation of tumor uptake was performed in terms of TBR as well as by calculating the relative tumor uptake posttreatment compared with baseline (TR). For this purpose, several circular ROIs with similar pixel size were automatically drawn using a computerized processing (Sophy NXT, Sopha Medical). The ROIs were initially defined on the posttreatment images when an apoptotic signal was localized at the tumor sites. In a second step, these ROIs were translated on the same anatomical sites on the pretreatment images. Practically, in cases of increased Annexin V uptake after chemotherapy, the number of counts obtained for tumor-bearing Annexin V was successively noted for each ROI [*i.e.*, ROI_1 (tumor signal posttreatment) = 16,000 counts and ROI_2 (similar tumor site pretreatment) = 8,000 counts]. Thereby, allowing us to calculate the TR (*i.e.*, $ROI_1/ROI_2 = 2$). Additional ROIs were also

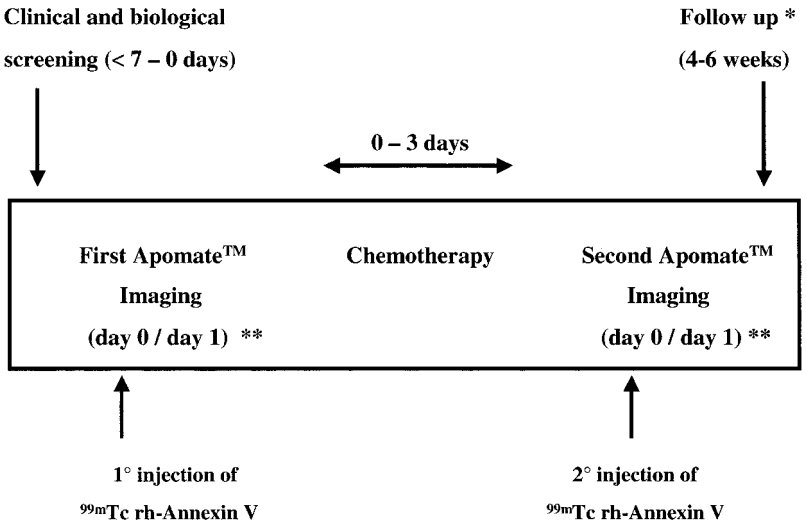

Fig. 1 Protocol design. ∗, the follow-up evaluation included physical examination, thoracic CTs, and whole body ^{18}FDG PET scans. ∗∗, day 0 = the day of injection of the apoptosis agent; day 1 = the 24th h after the injection of the apoptosis agent.

defined in areas free of tracer uptake [*i.e.,* ROI_3 (tumor signal posttreatment) = 16,000 counts and ROI_4 (lung background posttreatment) = 4,000 counts]. The TBR was then determined (*i.e.,* TBR = ROI_3/ROI_4 = 4). Otherwise, for the negative studies, no ROI was drawn. Overall, the change in tumor uptake of Apomate on posttreatment as compared with pretreatment images were graded as: grade 0: no change in uptake or a decrease in uptake posttreatment; grade 1: 10–50% increase in uptake posttreatment; grade 2: 50–100% increase in uptake posttreatment; grade 3: 100–200% increase in uptake post treatment; and grade 4: >200% increase in uptake posttreatment.

Conventional Anatomical Imaging. All patients were explored before and after chemotherapy by thoracic CT with contrast agent. CTs were performed using a PQ 2000 fourth generation (Picker, Cleveland, OH). In accordance with study enrollment criteria, all patients demonstrated at least one bidimensionally measurable tumor lesion (primary site and/or metastases) with diameters ≥1 cm.

Metabolic ^{18}FDG PET Imaging. Whole body PET was performed 1 h after i.v injection of 4–6 mCi of ^{18}FDG in 14 patients before chemotherapy and in all patients (n = 15) during follow-up. PET scans were performed using either a Penn Pet 240H scanner (UGM, Philadelphia, PA) or a C-Pet scanner (ADAC; Philips Medical Systems, Milpitas, CA).

Efficacy Assessment and Response Criteria. In all cases, tumor response to chemotherapy was evaluated in routine clinical fashion, including the CT and PET evaluations. In particular, the longest diameters of tumors measurable on posttreatment CT were compared with baseline pretreatment measurement. Patients were classified as having complete or PR and PD as indicated in Table 3. The median follow-up in this prospective study was 117 days (47–356 days).

Statistical Analysis. Qualitative results, suggesting or not an apoptotic signal after chemotherapy at tumor sites, were inferred from the visual comparison of the Annexin V-Tc^{99m} images immediately pre- and posttreatment (as detailed above). Quantitative results (TBR, TR) were expressed as mean and SD. Mean values were compared using the Student's t test when the distribution was normal and by Wilcoxon signed rank test otherwise.

The relationship of survival time to the ^{99m}Tc-Annexin V uptake (positive or negative) was estimated using the Kaplan-Meier method. The log rank test was used to compare the equality of survival curves. The degree of response to chemotherapy (CR, PR, and PD) was also appreciated in comparison to nuclear image data grading (Grade 0 to Grade 4) using Fisher's exact test for contingency tables and for assessing the dependence between categorical variables. In addition, a linear effect between the nuclear image grading and the response to tumor therapy was analyzed using Mantel-Haenszel's χ^2 test. All statistical results were considered to be significant at the 5% critical level ($P < 0.05$). All calculations were performed using SAS (version 6.12 for Windows) and S-PLUS 2000.

Results

Thirteen patients received two doses of ^{99m}Tc-Annexin V immediately before chemotherapy and within 3 days after completing the first course of treatment. Two patients received only one injection of Apomate after chemotherapy because of the urgency of treatment.

On prechemotherapy images, no ^{99m}Tc-Annexin V uptake was noted in tumors. Immediately before treatment, the patients only showed a similar nonpathologic biodistribution of radiotracer with uptake in salivary glands, liver, spleen, bone marrow, colon, kidneys, and bladder. On images obtained within 72 h after completing the first course of antitumor therapy, 7 patients (1 NHL, 1 HL, 2 SCLC, and 3 NSCLC) demonstrated a ^{99m}Tc-Annexin V uptake at the sites of primary or metastatic tumors. These sites were predominantly detected in regions of metastatic lymph nodes (cervical, mediastinal, and hilary nodes). Additionally, 3 patients also had a lung localization (1 NHL and 2 SCLC) and a rib uptake (1 NSCLC). Overall, 5 patients (1 NHL, 1HL, 1 SCLC, and 2 NSCLC) had a significant uptake 24 h after the radiopharmaceutical injection (P = 0.02), corresponding to the 48th h after completion of the first course

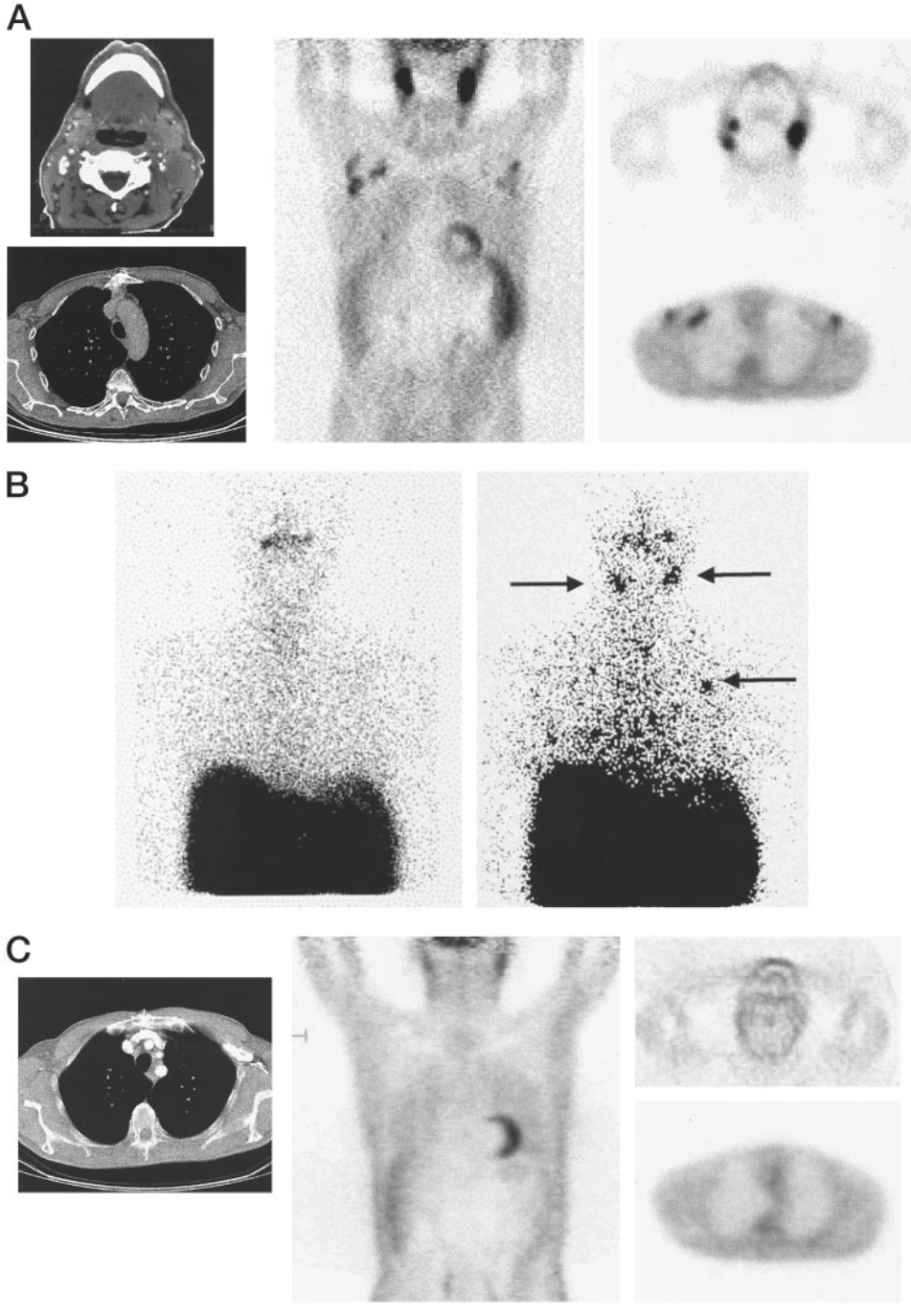

Fig. 2 A case of NHL (stage IV) treated by cyclophosphamide-doxorubicine-vincristine-prednisone protocol with a positive ^{99m}Tc-Annexin V study. *A*, the CTs of the neck and of the thorax (*left*) and the ^{18}FDG PET scan (*middle* and *right*) performed before treatment showed a lymph node dissemination at the cervical and axillary levels. *B*, the Annexin V imaging performed immediately before (*left*) and 48 h after chemotherapy (*right*) demonstrated an increased uptake of the apoptosis agent at the tumor sites (*arrows*). *C*, the posttreatment evaluation by the CTs and PET showed complete disappearance of disease.

of chemotherapy, whereas 2 patients (1 NSCLC and 1 SCLC) presented with a more intense ^{99m}Tc-Annexin V uptake 4 h after injection. The quantitative evaluation of tumor uptake in terms of TBR and TR confirmed the qualitative evaluation of the images in 6 of 7 patients having obvious tracer uptake at their tumor sites after chemotherapy. In 1 case of HL presenting with a large cervical mass, the visual interpretation showed diffuse faint uptake, whereas the TBR and TR ratios significantly differed before and after chemotherapy.

Among the 7 patients presenting with an increased Annexin V-Tc^{99m} uptake early after chemotherapy, 4 of them had CR (1 NHL, 1 HL, 1 NSCLC, and 1 SCLC) and the other 3 patients (2 NSCLC and 1 SCLC) had PR. On the basis of the CT and PET evaluations, all tumor sites with grade 3 and grade 4 ^{99m}Tc rh-Annexin V uptake completely disappeared after chemotherapy (Fig. 2), whereas the subjects with grade 1 and grade 2 uptake had partial response to treatment. On the other hand, 6 of 8 patients without Annexin V tumor uptake (grade 0) after

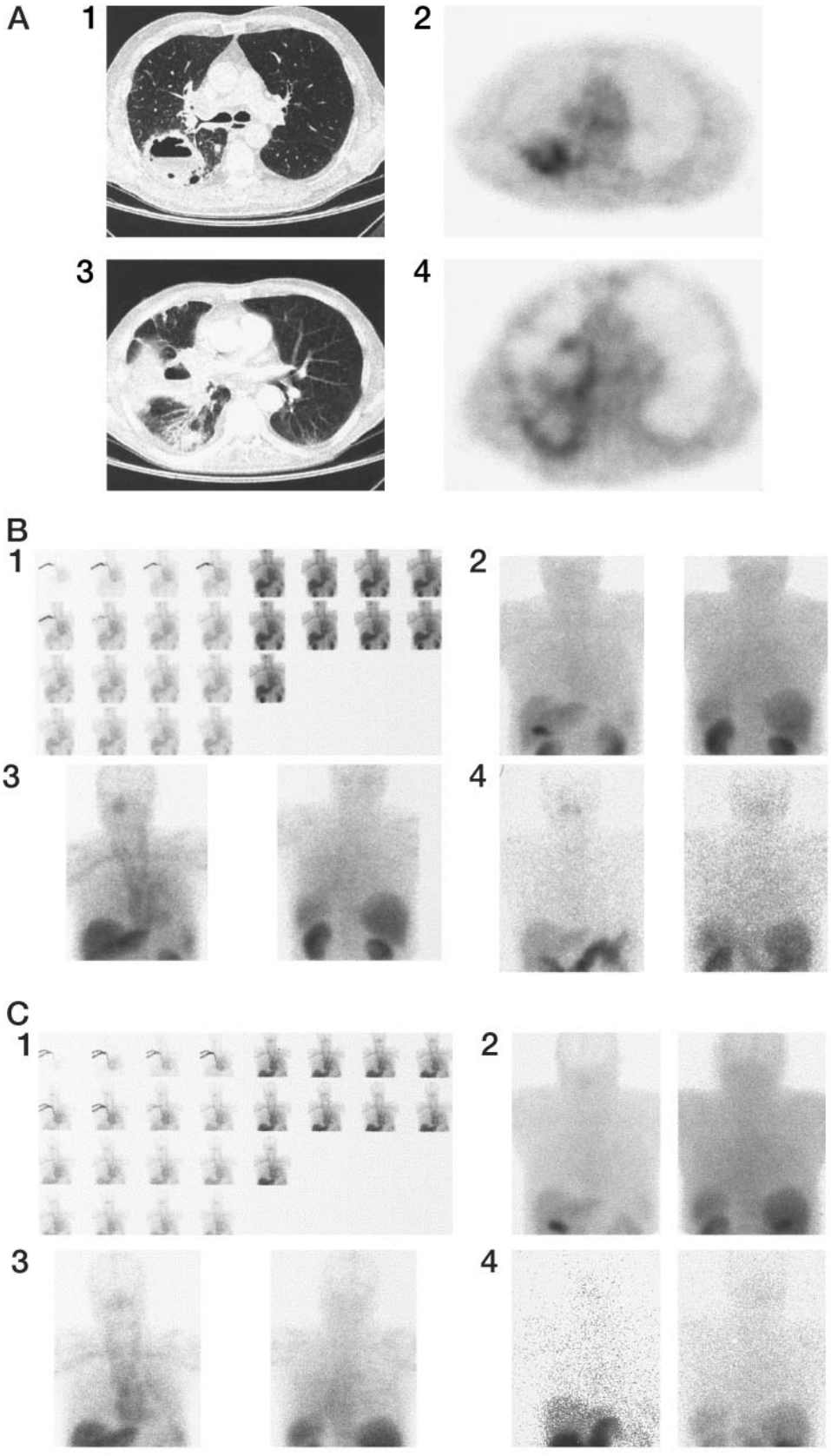

Fig. 3 A case of NSCLC (stage IV) treated by mitomycin-ifsofamide-*cis*-platinum protocol with a negative ^{99m}Tc-Annexin V study. *A*, thoracic CT and ^{18}FDG PET pretreatment **(**1 and 2**)** compared with posttreatment evaluation (3 and 4) showing an obvious progression of tumor. *B*, first Annexin V imaging performed immediately before chemotherapy with dynamic sequences (1, *top left*) and static anterior and posterior views at 15 min (2, *top right*), 4 h (3, *bottom left*), and 24 h (4, *bottom right*) after i.v. injection of the apoptosis agent. *C*, second Annexin V imaging performed immediately after chemotherapy with the same protocol showing no tumor uptake but the physiological distribution of tracer (liver, spleen, and colon).

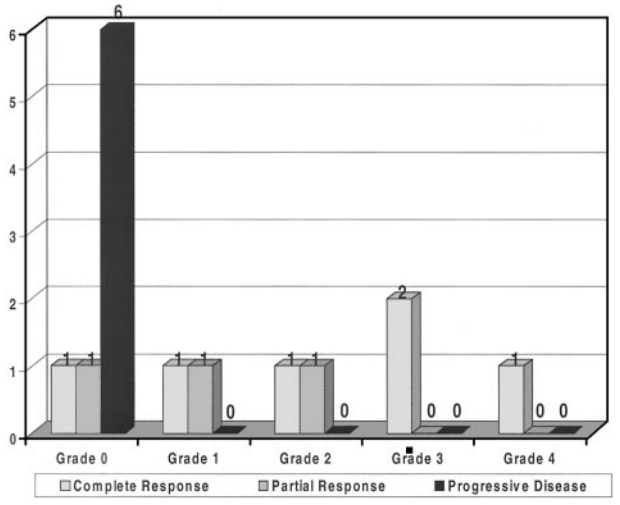

Fig. 4 Nuclear image grading correlated with the tumor response to chemotherapy. A statistical significance was observed in both Fisher's exact test ($P = 0.043$) and Mantel-Haenszel's χ^2 test ($P = 0.007$).

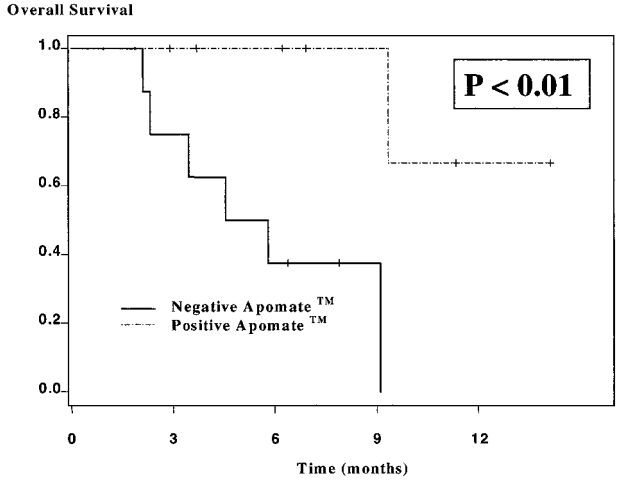

Fig. 5 Overall survival time of patients correlated with the Apomate results using the Kaplan-Meier method. $P < 0.01$ in log rank test.

chemotherapy (4 NSCLC, 2 BC, 1 SCLC, and 1 NHL) had PD (Fig. 3). Of them, 4 patients (4 of 6) died after a median follow-up of 3 months (64–138 days). Despite the lack of significant tracer uptake after chemotherapy, two cases of breast cancer had, however, complete and partial response to Taxol, respectively. Statistically, the tumor uptake of ^{99m}Tc-Annexin V was significantly correlated with the patient outcomes in terms of tumor response to chemotherapy and survival (Figs. 4–6). The results of the Annexin V imaging are detailed in Table 2.

And last but not least, no serious adverse events associated with ^{99m} Tc-Annexin V administration were observed, with a median follow-up of 4 months. In particular, no physical, biological, and hematological changes, including the coagulation tests related to the ^{99m} Tc-Annexin V administration, were noted. However, 1 patient (case 6 in Table 2)

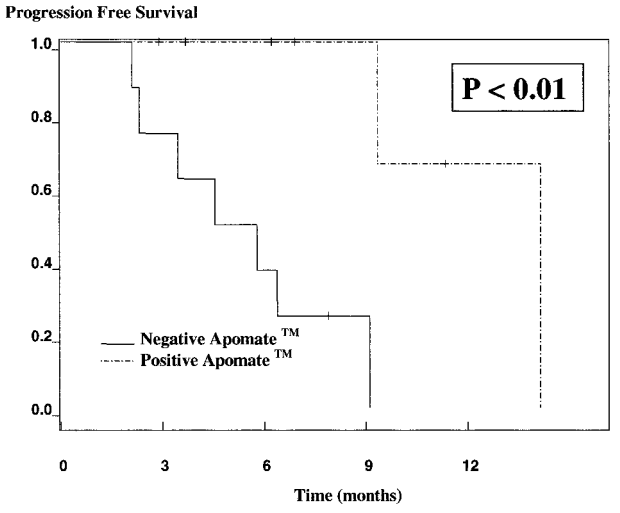

Fig. 6 Progression-free survival time of patients correlated with the Apomate results using the Kaplan-Meier method. $P < 0.01$ in log rank test.

presented a mild reaction 15 min after the second injection of ^{99m} Tc-Annexin V (after chemotherapy) corresponding to a facial rash, which regressed spontaneously 1 h later without any treatment. This patient was still in CR at his last follow-up (76 days).

Discussion

Most anticancer drug agents as diverse as topoisomerase inhibitors, alkylating agents, antimetabolites, and hormone antagonists generate apoptosis in sensitive cells (23–25). The genetic measurement of individual components of the apoptotic pathway does not necessarily reflect the functional ability of a tumor cell to commit to apoptosis in response to chemotherapy triggering. Mutations of *p53*, for instance, block the induction of apoptosis by various chemotherapeutic drugs in many cell types, whereas newer anticancer agents such as topoisomerase poisons, particularly topoisomerase I inhibitors, are able to induce apoptosis in many cells that lack functional *p53* (26, 27). In this study, we evaluated the technical feasibility and the clinical interest of ^{99m}Tc rh-Annexin V for noninvasively assessing the apoptotic functional capacity of treated tumors on a patient-by-patient basis.

Preclinical studies have shown that Annexin V binds tightly to PS. PS is a phospholipid normally expressed on the inner leaflet of the bilamellar cell membrane and is invariably translocated to the outer surface as an early event in apoptosis. i.v. administered ^{99m}Tc rh-Annexin V has been shown in preclinical and clinical studies to bind to externalized PS on apoptotic and necrotic cells with high avidity. Thus, ^{99m}Tc rh-Annexin V uptake suggests cellular apoptosis or necrosis. Blankenberg and Strauss (7–14) showed the potential of ^{99m}Tc rh-Annexin V for *in vivo* imaging of Fas-mediated fulminant hepatic apoptosis, chemotherapy-induced apoptosis in normal bone marrow and treated murine lymphoma, as well as in association with cardiac and lung allograft rejection and in hypoxic-ischemic cerebral reperfusion. Recently, in 7 patients

Table 2 Results from the Apomate study

Cases	Apomate grading	ΔTBR[a] 4 h/24 h	ΔTR 4 h/24 h	Annexin V-rh-Tc^{99m} uptake	Clinical response	Follow-up (days)
1	Grade 0	No uptake	No uptake	None	Died	64
2	Grade 3	1.7/2.0	0.6/2.8	Neck, mediastinum, hilum	CR	356
3	Grade 4	1.4/1.7	1.6/3.2	Neck, axilla, hilum	CR	345
4	Grade 0	No uptake	No uptake	None	Died	70
5	Grade 0	No uptake	No uptake	None	Died	105
6	Grade 0	No uptake	No uptake	None	PR	76
7	Grade 1	1.7/18.6	0.9/8.9	Mediastinum	PR	85
8	Grade 0	No uptake	No uptake	None	PR	124
9	Grade 2	1.6/0.9	1.8/1.2	Right rib	PR	85
10	Grade 0	No uptake	No uptake	None	Died	138
11	Grade 0	No uptake	No uptake	None	PD	99
12	Grade 0	No uptake	No uptake	None	PD	60
13	Grade 1	0.7/1.5	1.1/2.9	Neck (left area)	CR	58
14	Grade 2	2.4/1.7	NA	Hilum, mediastinum	PR	51
15	Grade 3	2.3/2.0	3.7/0.6	Hilum, mediastinum	CR	47

[a] ΔTBR (mean values), tumor-to-background ratios posttreatment (4 *versus* 24 h); ΔTR (mean values), relative tumor ratios posttreatment *versus* pretreatment (4 and 24 h); NA, not available because the patient had a single posttreatment Annexin V imaging because of the urgency of treatment.

presenting with documented acute myocardial infarction, Hofstra *et al.* (15) reported the feasibility of the radiolabeled Annexin V for the *in situ* imaging of necrosis and/or apoptosis. Similarly, in a series of 18 cardiac allograft recipients, Narula *et al.* (16) demonstrated the capability of the apoptosis imaging agent for noninvasive detection of transplant rejection confirmed by terminal deoxynucleotidyl transferase-mediated nick end labeling and/or caspase-3 (an apoptosis-specific proteolytic enzyme) immunohistochemical staining.

In oncology patients, the ability of tumor cells to respond apoptotically to chemotherapy varies from one tissue to another. In lymphomas, for instance, various treatments have shown to be efficient via chemotherapy-induced apoptosis in target tumor cells (28–31). This is one reason why this group of patients should be a priori good candidates for Annexin V imaging to assess the early apoptotic response of individual lymphomas to treatment. Indeed, 2 of 3 lymphoma patients studied in this series showed uptake of the imaging agent, suggesting their tumors had apoptotic capacity and both demonstrated objective clinical response to treatment. The third patient with a NHL showed no tracer uptake after treatment and had PD.

On the other hand, in untreated primary lung cancer, a previous work has indicated that the incidence of apoptosis known as the AI can vary widely (32). Histological analysis of 134 cases of NSCLC showed a mean AI of 0.3% (range, 0.02–1.4%), which was not correlated with the stage of disease, the degree of nodal involvement, the grade of tumor differentiation, or the differences in ploidy. Thus, the lack of significant pretreatment ^{99m}Tc rh-Annexin V uptake in NSCLC suggests that the planar imaging technique used in this study cannot routinely detect only 0.3% apoptosis. Nonetheless, in our series, pretreatment images were obtained as a control to compare with posttreatment uptake of the imaging agent.

Similar AI data on untreated primary tumors exist for patients with breast cancer. Studies from 105 women with invasive breast cancer have shown most of the specimens from untreated patients had $<1\%$ apoptosis (33). Although no uptake of ^{99m}Tc rh-Annexin V was seen in the 2 breast cancer patients enrolled in this series, both patients had partial clinical responses. The reason for the lack of tracer uptake visualized on imaging is not clear but may be related to failure to optimize the time of imaging after treatment when AI would have been elevated. The limited spatial resolution of currently used gamma cameras must also be considered.

Despite initial promise, *in vitro* sensitivity testing of tumors has not proved practical for routine clinical applications. Immunohistological and/or cytological apoptotic indexes determination on needle biopsy specimens showed promising results but are invasive (34). Morphological imaging procedures such as CT or magnetic resonance imaging provide accurate topographical information about the tumor changes after treatment, but they are unable to predict the response to chemotherapy. Metabolic changes usually precede gross tumor changes. PET imaging has been proposed to assess tumor viability by using either a glucose analogue (^{18}FDG) or radiolabeled amino acids (^{11}C-methionine, ^{11}C-tyrosine) (35–37). However, PET performances for early imaging of the chemotherapy response can be impaired in some clinical situations by inherent biochemical and technical limitations. For instance, the possibility of cellular stunning in the first few weeks after chemotherapy, resulting in false negative results, must be considered (38).

Our preliminary results demonstrated the ability of ^{99m}Tc rh-Annexin V to localize at tumor sites immediately after the first course of chemotherapy in lung cancer and lymphoma. Biopsies were not performed in this series, and the mechanism of localization of the imaging agent must be inferred from: (*a*) the preclinical and clinical data showing histological evidence of ^{99m}Tc rh-Annexin V localization at sites of apoptosis and necrosis; (*b*) the lack of ^{99m}Tc rh-Annexin V tumor uptake immediately before treatment; (*c*) the objective clinical responses seen in all patients whose tumors demonstrated posttreatment ^{99m}Tc rh-Annexin V uptake; and (*d*) the lack of objective clinical response in 6 of 8 patients whose tumors failed to demonstrate posttreatment ^{99m}Tc rh-Annexin V uptake. For these reasons, the observations are consistent with the hypothesis that ^{99m}Tc rh-Annexin V localizes at regions of apoptosis and necrosis immediately after anticancer treatment in patients whose tumors are able to respond apoptotically to such treat-

ment. The optimal timing for scintigraphic imaging of apoptosis in this study was about 20–24 h after the second injection (48 h after chemotherapy). By taking in account the 6-h half-time of ^{99m}Tc, the blood clearance of the ^{99m}Tc rh-Annexin V, as well as the counting statistics required for an adequate quality of the images, the acquisition protocol that appears the most flexible for the patient and the most efficient for imaging apoptosis after one course of treatment includes: static spot views of the thorax (anterior and posterior views) at 3–6 and 24 h after injection. Also, SPECT acquisition should probably be performed at 3–6 h after i.v. injection to improve the accuracy of detection.

This study demonstrated an excellent positive predictive value of ^{99m}Tc rh-Annexin V imaging in NSCLC and lymphoma that warrants additional larger multicentric studies to assess *in vivo* the apoptotic capacity of tumors by using the apoptosis imaging agent and, consequently, tumor response to therapy on patient-by-patient basis. Although promising, the results must be, however, interpreted cautiously. The heterogeneity of the histological nature of the tumors explored, as well as the heterogeneity of the drugs administrated, could explain some of the differences of tumor behavior observed. Prospective studies based on more homogeneous groups of patients in terms of histology and drugs protocol will be useful to evaluate more objectively the value of ^{99m}Tc-Annexin V for imaging apoptosis in human tumors.

In conclusion, the preliminary results of a Phase I study demonstrated the feasibility and the safety of ^{99m}Tc-Annexin V for localizing apoptosis in treated human tumors, particularly in lymphomas and late stage lung cancers. The selective *in situ* detection of the apoptotic signal is possible, as early as 1 day after the first course of chemotherapy. The determination of apoptotic competence of human tumors via their actual apoptotic response to therapy using a noninvasive and reproducible imaging tool could have important clinical implications in cancer management.

Additional clinical trials based on larger multicentric series remain, however, necessary before the introduction of the technique in oncology practice.

Acknowledgments

We thank Marybeth Mallett for helpful assistance.

References

1. Kerr, J. F., Wyllie, A. H., and Currie, A. R. Apoptosis: a basic biological phenomenon with wide-ranging implications in tissue kinetics. Br. J. Cancer, *26:* 239–257, 1972.

2. Evan, G. I., and Vousden, K. H. Proliferation, cell cycle, and apoptosis in cancer. Nature (Lond.), *411:* 342–348, 2001.

3. Harrington, E. A., Fanidi, A., and Evan, G. I. Oncogenes and cell death. Curr. Opin. Genet. Dev., *4:* 120–129, 1994.

4. Darzynkiewicz, Z. Apoptosis in antitumor strategies: modulation of cell cycle or differentiation. J. Cell. Biochem., *58:* 151–159, 1995.

5. Lennon, S. V., Martin, S. J., and Cotter, T. G. Dose-dependent induction of apoptosis in human tumour cell lines by widely diverging stimuli. Cell Prolif., *24:* 203–214, 1991.

6. Martin, S. J., Reutelingsperger, C. P., McGahon, A. J., Rader, J. A., van Schie, R. C., LaFace, D. M., and Green, D. R. Early redistribution of plasma membrane phosphatidylserine is a general feature of apoptosis regardless of the initiating stimulus: inhibition by over expression of Bcl-2 and Abl. J. Exp. Med., *182:* 1545–1556, 1995.

7. Ogura, Y., Krams, S. M., Martinez, O. M., Kopiwoda, S., Higgins, J. P., Esquivel, C. O., Strauss, H. W., Tait, J. F., and Blankenberg, F. G. Radiolabeled annexin V imaging: diagnosis of allograft rejection in an experimental rodent model of liver transplantation. Radiology, *214:* 795–800, 2000.

8. Vriens, P. W., Blankenberg, F. G., Stoot, J. H., Ohtsuki, K., Berry, G. J., Tait, J. F., Strauss, H. W., and Robbins, R. C. The use of technetium Tc 99m annexin V for *in vivo* imaging of apoptosis during cardiac allograft rejection. J. Thorac. Cardiovasc. Surg., *116:* 844–853, 1998.

9. Blankenberg, F. G., Robbins, R. C., Stoot, J. H., Vriens, P. W., Berry, G. J., Tait, J. F., and Strauss, H. W. Radionucleide imaging of acute lung transplant rejection with annexin V. Chest, *117:* 834–840, 2000.

10. Blankenberg, F. G., Ohtsuki, K., Tait, J., and Strauss, H. W. Apoptosis: the importance of nuclear medicine. Nucl. Med. Commun., *21:* 241–250, 2000.

11. Ohtsuki, K., Akashi, K., Aoka, Y., Blankenberg, F. G., Kopiwoda, S., Tait, J. F., and Strauss, H. W. Technetium-99m HYNIC-annexin V: a potential radiopharmaceutical for the *in vivo* detection of apoptosis. Eur. J. Nucl. Med., *26:* 1251–1258, 1999.

12. Blankenberg, F. G., Katsikis, P. D., Tait, F., Davis, R. E., Naumovski, L., Ohtsuki, K., Kopiwoda, S., Abrams, M. J., and Strauss, H. W. Imaging of apoptosis (programmed cell death) with 99mTc annexin V. J. Nucl. Med., *40:* 184–191, 1999.

13. D'Arceuil, H., Rhine, W., de Crespigny, A., Yenari, M., Tait, J. F., Strauss, W. H., Engelhorn, T., Kastrup, A., Moseley, M., and Blankenberg, F. G. ^{99m}Tc annexin V imaging of neonatal hypoxic brain injury. Stroke, *31:* 2692–2700, 2000.

14. Blankenberg, F. G., Naumovski, L., Tait, J. F., Post, A. M., Strauss, H. W. Imaging cyclophosphamide-induced intramedullary apoptosis in rats using 99mTc-radiolabeled annexin V. J Nucl Med., *42:* 309–316, 2001.

15. Hofstra, L., Liem, I. H., Dumont, E. A., Boersma, H. H., van Heerde, W. L., Doevendans, P. A., De Muinck, E., Wellens, H. J., Kemerink, G. J., Reutelingsperger, C. P., and Heidendal, G. A. Visualisation of cell death *in vivo* in patients with acute myocardial infarction. Lancet, *356:* 209–212, 2000.

16. Narula, J., Acio, E. R., Narula, N., Samuels, L. E., Fyfe, B., Wood, D., Fitzpatrick, J. M., Raghunath, P. N., Tomaszewski, J. E., Kelly, C., Steinmetz, N., Green, A., Tait, J. F., Leppo, J., Blankenberg, F. G., Jain, D., and Strauss, H. W. Annexin-V imaging for noninvasive detection of cardiac allograft rejection. Nat. Med., *7:* 1347–1352, 2001.

17. Zwaal, R. F., and Schroit, A. J. Pathophysiologic implications of membrane phopholipid asymmetry in blood cells. Blood, *89:* 1121–1132, 1997.

18. Cookson, B. T., Engelhardt, S., Smith, C., Bamford, H. A., Prochazka, M., and Tait, J. F. Organization of the human annexin V (ANX5) gene. Genomics, *20:* 463–467, 1994.

19. Huber, R., Berendes, R., Burger, A., Schneider, M., Karshikov, A., Luecke, H., Romisch, J., and Pâques, E. Crystal and molecular structure of human annexin V after refinement. Implications for structure, membrane binding and ion channel formation of the annexin family of proteins. J. Mol. Biol., *223:* 683–704, 1992.

20. Pigault, C., Follenius-Wund, A., Schmutz, M., Freyssinet, J. M., and Brisson, A. Formation of two-dimensional arrays of annexin V on phosphatidylserine-containing liposomes. J. Mol. Biol., *236:* 199–208, 1994.

21. Meers, P., and Mealy, T. Relationship between annexin V tryptophan exposure, calcium, and phospholipid binding. Biochemistry, *32:* 5411–5418, 1993.

22. Kasina, S., Rao, T. N., Srinivasan, A., Sanderson, J. A., Fitzner, J. N., Reno, J. M., Beaumier, P. L., and Fritzberg, A. R. Development and biologic evaluation of a kit for preformed chelate technetium-99m radiolabeling of an antibody Fab fragment using a diamide dimercaptide chelating agent. J. Nucl. Med., *32:* 1445–1451, 1991.

23. Hickman, J. A. Apoptosis induced by anticancer drugs. Cancer Metastasis Rev., *11:* 121–139, 1992.

24. Dive, C., Evans, C. A., and Whetton, A. D. Induction of apoptosis: new targets for cancer chemotherapy. Semin. Cancer Biol., *3:* 417–427, 1992.

25. Lowe, S. W., and Lin, A. W. Apoptosis in cancer. Carcinogenesis (Lond.), *21:* 485–495, 2000.

26. Murakami, Y., Hayashi, K., Hirohashi, S., and Sekiya, T. Aberrations of the tumor suppressor p53 and retinoblastoma genes in human hepatocellular carcinomas. Cancer Res., *51:* 5520–5525, 1991.

27. Lowe, S. W. Cancer therapy and p53. Curr. Opin. Oncol., *7:* 547–553, 1995.

28. Weiss, L. M., Warnke, R. A., Sklar, J., and Cleary, M. L. Molecular analysis of the t(14;18) chromosomal translocation in malignant lymphomas. N. Engl. J. Med., *317:* 1185–1189, 1987.

29. Vaux, D. L., Cory, S., and Adams, J. M. *Bcl-2* gene promotes haemopoietic cell survival and cooperates with c-myc to immortalize pre-B cells. Nature (Lond.), *335:* 440–442, 1988.

30. Maloney, D. G., Smith, B., and Appelbaum, F. R. The anti-tumor effect of monoclonal anti-CD20 antibody therapy includes direct anti-proliferative activity and induction of apoptosis in CD20 positive non-Hodgkin's lymphoma cell lines (Abstract). Blood, *88* (Suppl. 1)*:* 637a, 1996.

31. Demidem, A., Lam, T., Alas, S., Hariharan, K., Hanna, N., and Bonavida, B. Chimeric anti-CD20 (IDEC-C2B8) monoclonal antibody sensitizes a B cell lymphoma cell line to cell killing by cytotoxic drugs. Cancer Biother. Radiopharm., *12:* 177–186, 1997.

32. Ghosh, M., Crocker, J., and Morris, A. Apoptosis in squamous cell carcinoma of the lung: correlation with survival and clinicopathological features. J. Clin. Pathol., *54:* 111–115, 2001.

33. Gonzalez-Palacios, F., Sancho, M., Martinez, J. C., and Bellas, C. Microvessel density, p53 overexpression, and apoptosis in invasive breast carcinoma. Mol. Pathol., *50:* 304–309, 1997.

34. Allen, R. T., Hunter, W. J., III, and Agrawal, D. K. Morphological and biochemistry characterization and analysis of apoptosis. J. Pharmacol. Toxicol. Meth., *37:* 215–228, 1997.

35. Warburg, O. On the origin of cancer cells. Science (Wash. DC), *123:* 309–314, 1956.

36. Pauwels, E. K., Ribeiro, M. J., Stoot, J. H., McCready, V. R., Bourguignon, M., and Maziere, B. FDG accumulation and tumor biology. Nucl. Med. Biol., *25:* 317–322, 1998.

37. Delbeke, D. Oncological applications of FDG PET imaging. J. Nucl. Med., *40:* 1706–1715, 1999.

38. Bar-Shalom, R., Valdivia, A. Y., and Blaufox, M. D. PET imaging in oncology. Semin. Nucl. Med., *30:* 150–185, 2000.